EFFECT OF MULTIPLE HEAT SIMULATION ON A CGHAZ FRACTURE OF LOW CARBON LOW ALLOYED STEELS

A. BROŽOVÁ

Nuclear Research Institute Řež, plc.
25068 Řež, Czech republic

ABSTRACT

The paper presents a final report of project in framework of European Concern Action COST 517 – "Cleaner Metal to Industrial Exploitation". The project addresses an effect of alloy cleanness in a welding process. It is solved for a repair welding of pressure vessels made from two low-alloyed steels, CrNiMoV and CrMoV. An evolution of microstructure and mechanical and fracture behaviour of coarse grain HAZ of the weld repairs is studied.

Experimental testing using static, dynamic and impact toughness of simulated material structures showed relative quality of the local microstructural regions. The results are used for discussion of a possible effect of preheating to effect of cold cracking of a weld repairs. From the comparison of the two steels the worse weldability is reflected in worse fracture behaviour of base material and simulated states.

KEYWORDS

Weld repair, local brittle zone, fracture toughness

INTRODUCTION

The report concludes research work aimed to determine a cause of different weldability of repair welds and an occurrence of cold cracks in reactor pressure vessels (RPV) [1, 2].

The goal of the study was to search for a positive effect of preheating on the cold cracking occurrence. The effect was studied on two similar steels, CrMoV and CrNiMoV ferritic steels, one of them possessing worse weldability (CrMoV) than the other one. It was studied only the coarse grain heat affected zones (CGHAZ) of the both steels. The HAZ structures were prepared using a heat simulating technique. The primary CGHAZ and the secondary reheated CGHAZ structures (subcriticly reheated CGHAZ), SRCGHAZ, of MIG welding were simulated. The weldability of the steels was evaluated according fracture behaviour of HAZ structures.

The experimental program includes mechanical testing of the critical zones and microscopic observations of the microstructures and fractures.

EXPERIMENTAL

Materials

The base material steels of chemical composition included in Table 1 were used for the study. The test pieces were cut from commercial treated material pieces (forging, rolling and several heat treatments).

The steels exhibit microstructure of tempered bainite, Fig. 1 and 2.

Carbides, MnS and complex particles occurred in the both steels [3, 4]. Relatively higher amount of the particles possessed CrMoV steel than CrNiMoV steel. The particle distribution was measured by light microscopy. For CrMoV, the particles can be characterised by the mean area 0.2 - 0.07 % and the equivalent diameter 3 ± 2 mm (approximate round shape of particles) with maximum 24 mm, minimum 1 mm.

The results of Auger electron spectroscopic measurement of the intergranularly fractured base materials have shown traces of P and S segregation on grain boundaries of the CrMoV steel [5]. No segregation was detected in the CrNiMoV steel.

Table 1. Chemical composition of pressure vessel steels (mass %).

Steel	C	Mn	Si	P	S	Cr	Ni	Cu	Mo	V	As	d_A [μm]
CrMoV	0.21	0.42	0.23	0.012	0.01	2.76	0.14	0.08	0.66	0.32	0.009	120 ± 40
CrNiMoV	0.15	0.44	0.24	0.010	0.008	2.05	1.22	0.06	0.57	0.09	0.007	80 ± 10

d_A…austenite grain size

Weld heat cycles simulation

Heat simulations were realised using the SMITWELD apparatus. The welding of RPV was simulated by multiple bead MIG (MAG) method of heat input at transient (cushion) layer at weld metal 7 kJ/cm using ferritic, resp. austenitic welding rods. It was simulated weld repairing processes of RPV with and without preheating to 200°C. Heating rate was 100°C/hour and the period over 1200°C (temperature of intensive grain growth) was 3 - 4 s.

Table 2. Parameters of heat simulation cycles for the CrNiMoV and CrMoV steels.

	Preheat	Heat cycle periods, cooling part [s]				
State	[°C]	1350 - 800	800 - 500	500 - 300	300 - 200	200 - 50
B1	50	3.2	3.5	7	10	370
B2	200	3.2	6.6	27	358	-
C1	50	-	1.2*	7	10	370
C2	200	-	2.2*	27	358	-

* 650 – 500°C

Four different heat simulation cycles were applied as it is described in Table 2. Four microstructures were created using single and double cycles: B1, B1 + C1, B2 and B2 + C2. The double cycles are shortly assigned as C1 and C2 in the following text. The double cycles simulations are shown in following Fig. 3.

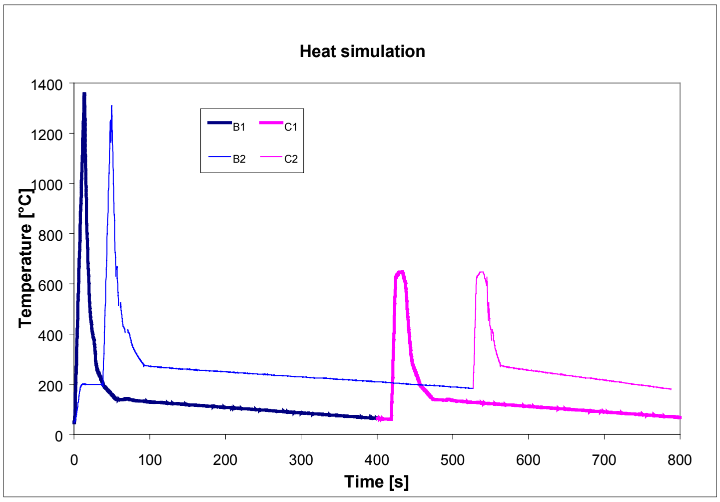

Fig. 3. Records of temperature vs. time course for heat simulation cycles B1, B2, C1 and C2. Notice different profiles in parts of the graph connecting to cooling between 600°C and 200°C.

After the heat simulation all the new microstructures were studied by light microscopy.

The heat simulation were applied on rectangular pieces of dimensions 11 x 11 x 70 mm used for the Charpy specimen machining and on circular pieces of diameter 4 mm and length 70 mm used for weldability tests.

Mechanical testing

Charpy specimens of 10 x 10 x 55 mm were manufactured from the simulated material pieces. One group of specimens were notched and tested by impact test at room temperature.

Second group of specimens were pre-fatigued and tested for dynamic fracture toughness, K_{Id}, vs. temperature curve.

The last group of specimens pre-fatigued and tested for J - R resistance curve at room temperature air.

RESULTS

Microstructures after heat simulations

After application of heat simulation of all the weld cycles (B1, B2, B1 + C1, B2 + C2) significant microstructural changes of all materials were observed. The microstructures of both steels changed from tempered bainite to martensite or martensite/bainite [9, 10]. In the case of CrNiMoV higher martensite content were reached.

Light microscopy (LM) disclosed only weak differences between the simulated states. Specification of the differences have to be studied using TEM [9]. Fig. 4 – 9 show different parts of the simulated microstructure representing states B1, C1 and C2. Fig 10 shows normal distribution of austenite grain size for the simulated states.

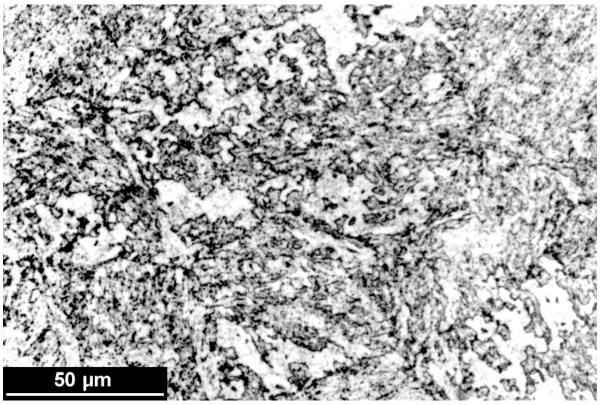

Fig. 1: Microstructure of CrNiMoV steel in base state - tempered bainite.

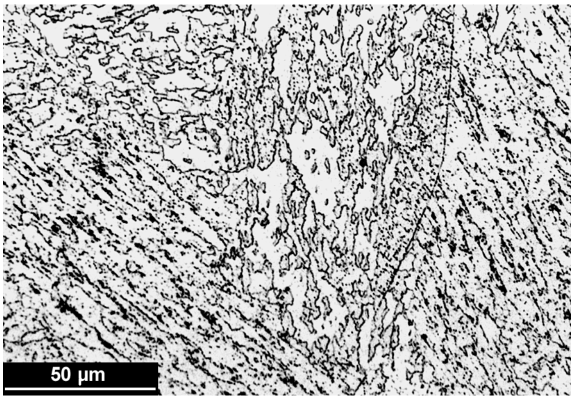

Fig. 2: Microstructure of CrMoV steel in base state - tempered bainite.

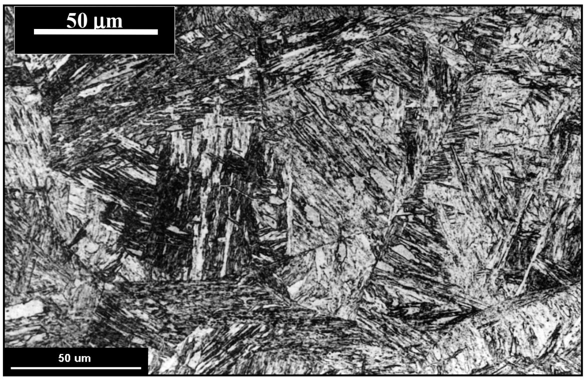

Fig. 4: CrNiMoV steel after B1 simulation.

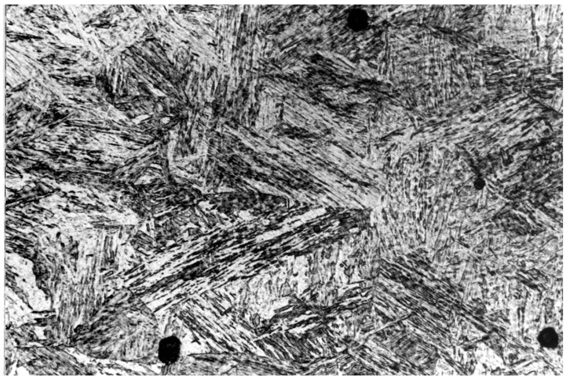

Fig. 5: CrMoV steel after B1 simulation.

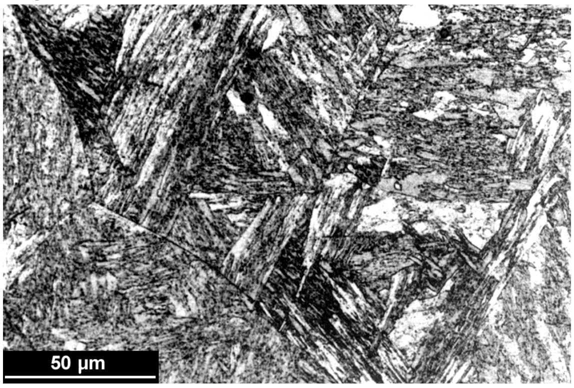

Fig. 6: CrNiMoV steel after C1 simulation.

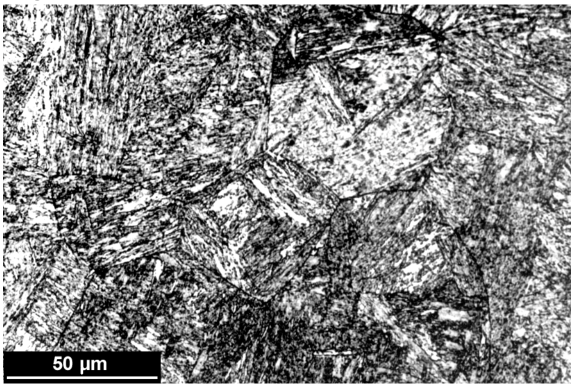

Fig. 7: CrMoV steel after C1 simulation.

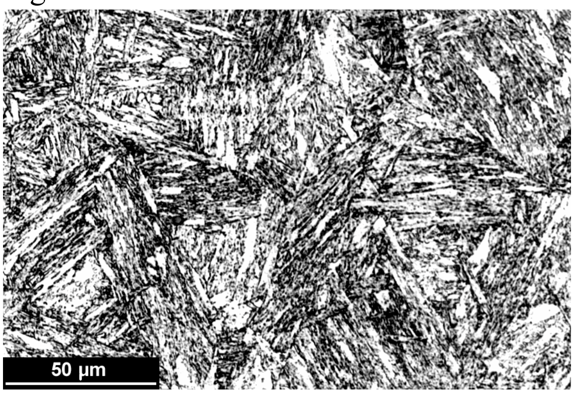

Fig. 8: CrNiMoV steel after C2 simulation.

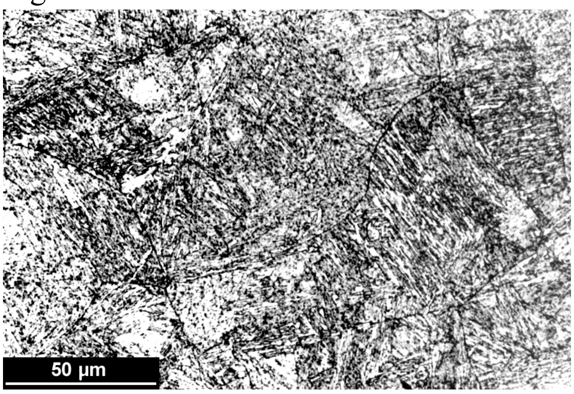

Fig. 9: CrMoV steel after C2 simulation.

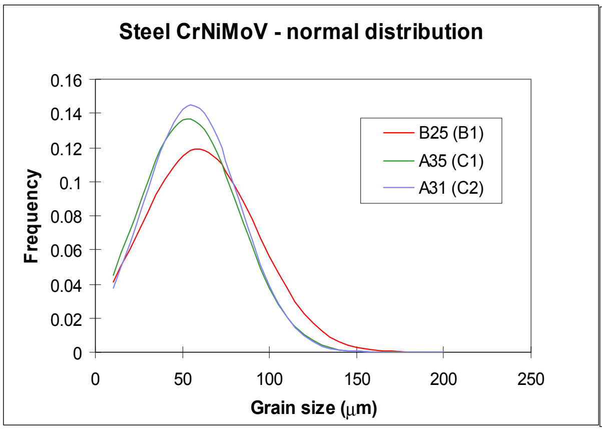

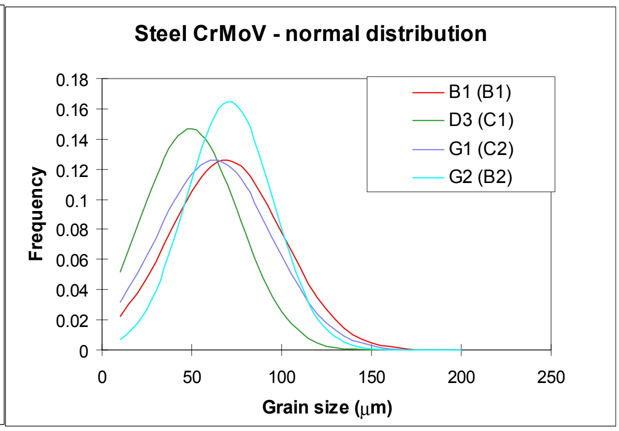

Fig. 10: Normal distribution of austenite grain size – calculated from LM data.

Mechanical tests

The results of the impact tests [11, 12] are shown in Fig. 11. Generally, the simulated structures of the CrMoV possessed lower values of the impact energy KCV and lower amount of ductile fracture were measured on the fracture surface. From the Figs it is clearly seen that the worst impact toughness properties were found in case of the C1 state for the both steels.

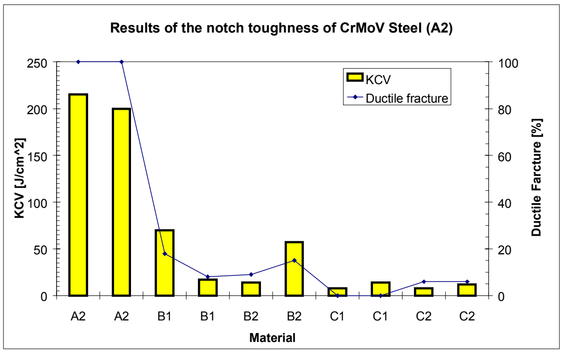

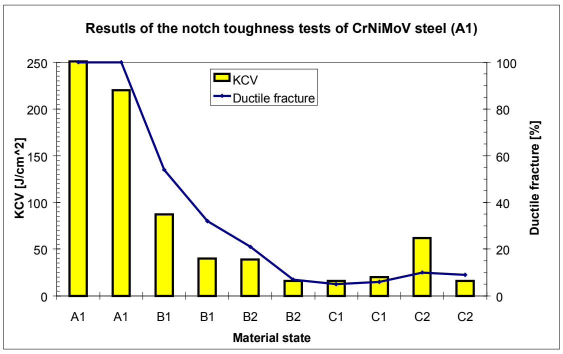

Fig. 11: Impact energy and percentage of ductile fracture on the fracture surface at room temperature of the simulated states and the base material.

The results of the dynamic fracture toughness measurements [13, 14] are shown in Fig. 12, 13. All the curves of the simulated states are shifted to higher temperatures. The highest transition temperatures on a level of 100 MPam$^{1/2}$ were evaluated for C1 in case of the CrNiMoV steel and for C1, C2 in the case of the CrMoV steel. The transition temperatures are higher than room temperature for the C states.

Another important result follows from the comparison of the two steels. For the CrNiMoV steel (Fig. 12) it can be observed that a significant shift of the K_{Id} transition curve occurred for all simulated states. For CrMoV steel the larger shift can be seen only for the C1, C2 states.

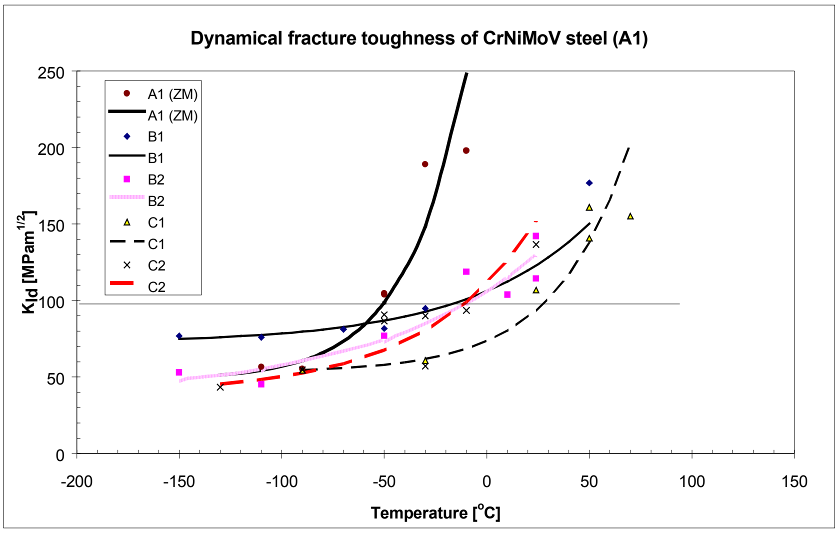

Fig. 12: Transition curves of the dynamic fracture toughness of the CrNiMoV steel simulated states and the base material.

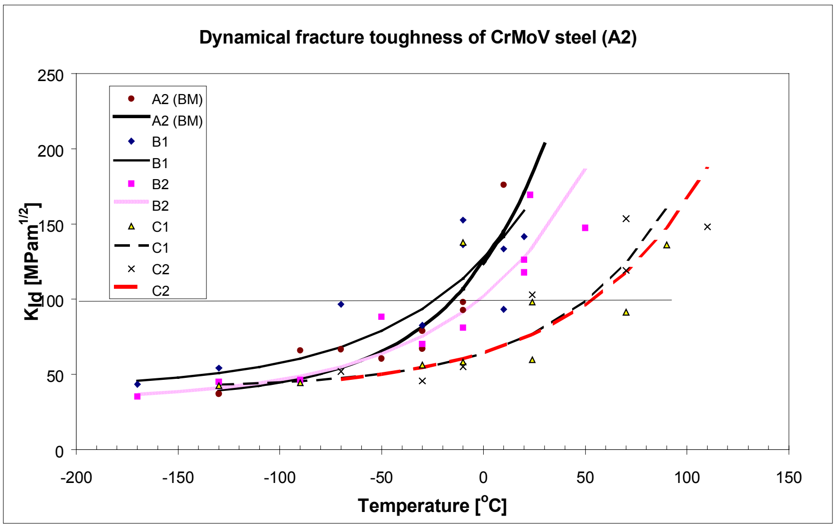

Fig. 13: Transition curves of the dynamic fracture toughness of the CrMoV steel simulated states and the base material.

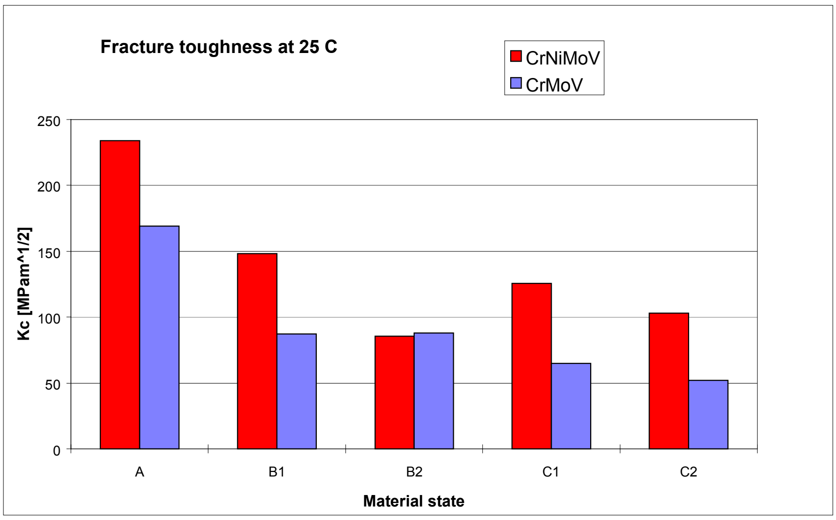

Fig. 14: Results of static fracture toughness of the CrMoV and CrNiMoV steels, simulated states and base materials.

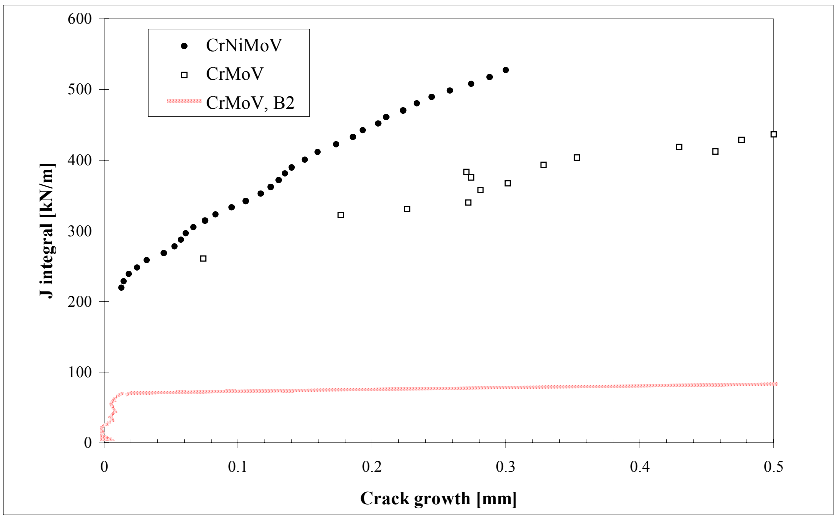

Fig. 15: J - R resistance curves measured at room temperature. Results of the two base materials, CrNiMoV and CrMoV steels and the one simulated state, B2, of the CrMoV steel.

For all the simulated states it was measured material values of fracture toughness K_C at room temperature, Fig 14. All the specimens fractured by unstable fracture after pop-ins of different amount. The behaviour is a typical one for a transition region.

The results of static resistance J - R curve measurement of the base materials and one simulated state B2 at room temperature are shown in Fig. 15. It is seen that CrMoV steel has lower ductile fracture resistance even in the base material state, where ductile fracture prevailed, Fig. 16 [15]. The ductility was lowered likely due to ductile intergranular fracture, Fig. 17 [15]. The B2 simulated state of CrMoV steel, fractured in the tests by pop-ins. The crack growth mechanism changed from ductile at stadium of stretch zone formation to unstable transgranular cleavage fracture after pop-in, Fig. 18 and 19 [15].

Another important feature of the RT static fracture was that very low T modulus was measured for the CGHAZ structures. It indicates very easy crack propagation in the HAZ materials.

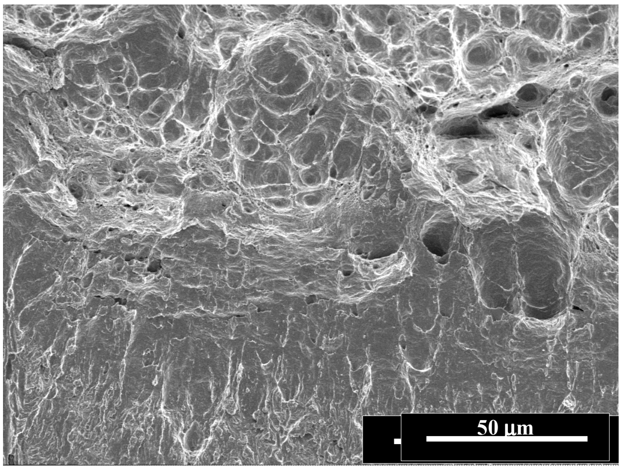

Fig. 16: Ductile stretch zone in CrMoV steel, after J integral test, RT (crack grew from bottom to top).

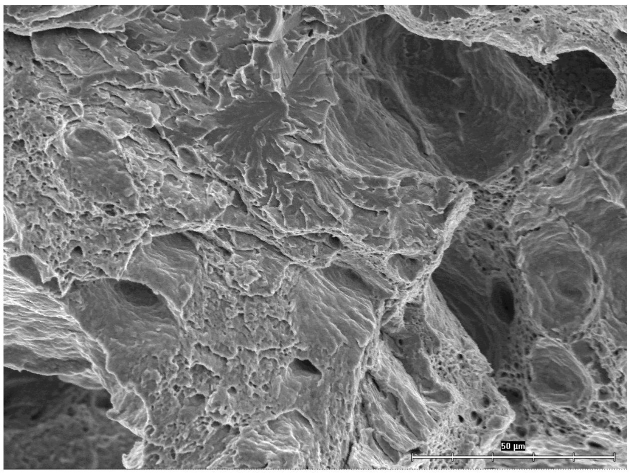

Fig. 17: CrMoV steel, detail of intergranular ductile fracture, J test, RT (crack grew from bottom to top).

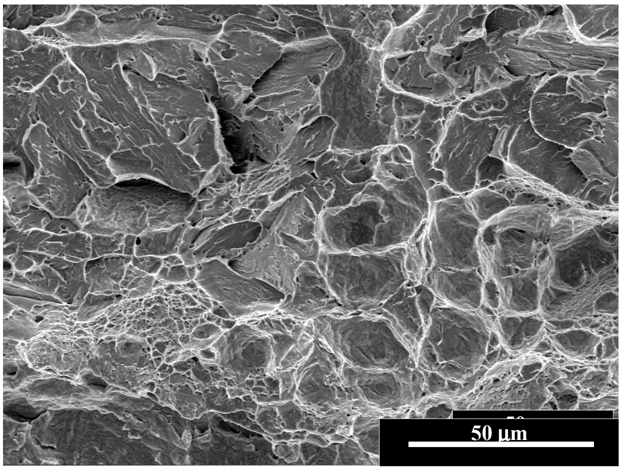

Fig. 18: Ductile crack increment followed by cleavage pop-in, CrMoV/B2, after J integral test, RT (crack grew from bottom to top).

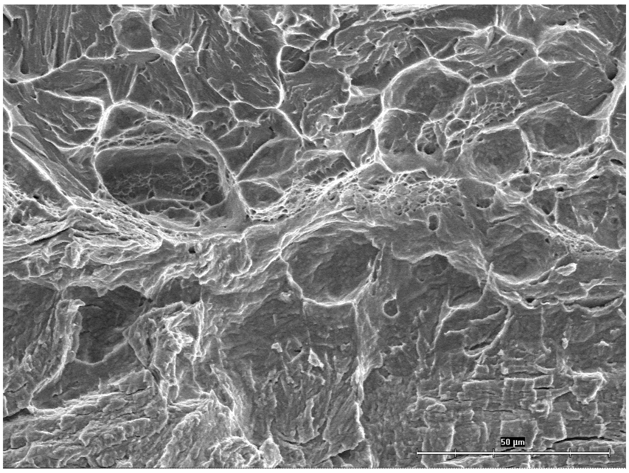

Fig. 19: Ductile stretch zone and small crack increment, CrMoV/B2, J integral test, RT (crack grew from bottom to top).

DISCUSSION

The mechanical testing results agree in general with the previous results of the simulated HAZ of the weld repairing [16]. After the primary heat cycle mechanical properties of the new microstructures degrade due to microstructural changes. The new, mainly martensite microstructures are of the high critical fracture stresses (about 3500 MPa) and of the high yield stresses. The combination means that plasticity of the material is very low and, therefore, the crack growth resistance decreases.

The better weldability of the CrNiMoV steel in comparison to the CrMoV steel can be seen clearly from the experimental results. It appears that the application of the C2 simulation on CrNiMoV steel produces the microstructure with improved fracture resistance than in the case of the C1 state. For the CrMoV steel, no difference is seen between the C1 and C2 fracture properties. It means that the preheating to 200°C was not sufficient to avoid the cold cracking propagation. It seems that not only the resistance of the local microstructure is important for the cold cracking process but also the resistance of the base metal surrounding it.

Implant tests, the classic tests of weldability, can give a first, rough picture of material quality in order to select steel of good weldability. But the test serves only for a relative material selection and a cause of the difference in material properties cannot be deduced. Using heat simulation technique [7, 8] important values for the repair welding process can be measured, i.e. phase transformation temperatures, possible residual stresses or strain characteristics of the weld joint. The values are typical for the welding and cannot be applied to another one.

Besides, the simulation technique can serve as a source of homogeneous material structures in large piece of material than can be found in a real weld joint. Due to a standard material behaviour can be measured for the HAZ structures.

CONCLUSIONS

Results of testing have shown that during repair welding of CrMoV and CrNiMoV steels with and without pre-heating

- Microstructures consisting of bainite / martensite mixture create in coarse grain HAZ. The CG HAZ materials possess low resistance to crack initiation and growth in static and dynamic fracture.
- The CG HAZ microstructures created during primary and secondary simulations differs in grain size distribution, the widest distribution was measured for both C2 microstructures.
- Effect of MnS particles on microstructures was not found

Comparing results of CrMoV and CrNiMoV steels it is evident that CrMoV posses lower fracture behaviour in all test categories – KCV, K_{IC}, K_{Id}.

The sensitivity to cold cracking results from a combination of a sensitivity to crack initiation, i.e. hydrogen effects, and low resistance to crack propagation. The tested pre-heating regime has only small effect on the cold cracking prevention. Results of the study have shown that even for CrNiMoV steel the pre-heating before repair welding cannot fully avoid the cold cracking.

ACKNOWLEDGEMENT

This work occurred in framework of the project granted by the COST Action 517 (Grant Nr. OC517.10). The support of the work is highly appreciated.

REFERENCES

[1] Bečka J., Report SKODA, Ae8825, 1997 (in Czech).
[2] Bečka J. et al., In: Proc. of 18th Congress of Welding Institute Bratislava, Tatranska Lomnica, 1989 (in Czech).
[3] Keilová E., Protokol 10/98, NRI Řež, 1998 (in Czech).
[4] Keilová E., Protokol 12/98, NRI Řež, 1998 (in Czech).
[5] Lejček P., unpublished results.
[6] Gliha V., Vuherer T., Report on Implant Testing, COST 517, University of Maribor, June 2000.
[7] Bečka J. et al., „Podklady pro dílčí závěrečnou zprávu úkolu COST 517“, December 2000 (in Czech).
[8] Šolc P., Bečka J., Protokol “Simulace svařovacích cyklů na přístroji SMITWELD TTU2002”, ŠKODA Výzkum, 1999 (in Czech).
[9] Keilová E., Kočik J., Protokol 13/98, NRI Řež, 1998 (in Czech).
[10] Keilová E., Kočik J., Protokol 6/99, NRI Řež, 1999 (in Czech).
[11] Falcník M., Protokol OMV NAL 98/10, NRI Řež, 1998 (in Czech).
[12] Falcník M., Protokol OMV NAL 98/31, NRI Řež, 1998 (in Czech).
[13] Falcník M., Protokol OMV NAL 99/42, NRI Řež, 1999 (in Czech).
[14] Falcník M., Protokol OMV NAL 99/43, NRI Řež, 1999 (in Czech).
[15] Burda J., unpublished results.
[16] Brozova A. et al., Engineering Mechanics 5 (3), 1998, p. 181 - 186.